ICASSP 2025 - 2025 IEEE International Conference on Acoustics, Speech and Signal Processing (ICASSP) | 979-8-3503-6874-1/25/$31.00 ©2025 IEEE | DOI: 10.1109/ICASSP49660.2025.10890749

Situation-aware Space-time Waveform Design for Automotive MIMO Radars

Edoardo Focante[1], Nitin Jonathan Myers[1], Geethu Joseph[1], Ashish Pandharipande[2]
[1]*Delft University of Technology, The Netherlands*
[2]*NXP Semiconductors, The Netherlands*
Email: {e.focante, n.j.myers, g.joseph}@tudelft.nl, ashish.pandharipande@nxp.com

***Abstract*—Radar is a key technology in automotive driving for target detection and perception. In this work, we leverage prior environmental information in the form of occupancy maps to design space-time codes for a fully digital MIMO radar. We transform this design problem into the optimization of spatial beamforming gains and time-domain codes. The beamforming gains are optimized to enhance the strength of returns from cells associated with a higher uncertainty of occupancy. The time-domain codes are optimized to minimize the correlation between returns of targets within the drivable space. We validate our method on the nuScenes dataset to show that the designed space-time codes achieve higher detection rates than designs that do not rely on prior information from occupancy maps.**

***Index Terms*—Automotive radar, situation-aware waveform design, occupancy grid maps.**

I. Introduction

Millimeter-wave radar is one of the main sensing modalities in current assisted and autonomous driving systems. Existing millimeter-wave multi-input multi-output (MIMO) radars have the ability to adapt the space-time codes applied at the transmitter. For instance, the beams at a radar transmitter or the time-domain codes can be designed using side information available on the environment being sensed. This side information can be in the form of an occupancy grid map [1]–[3]. An occupancy map is a grid of range-angle-Doppler cells, with the occupancy value in a cell being the probability that the cell is occupied by an object. A radar can adjust its transmitted waveform based on the information provided by the occupancy map.

Prior work leveraged occupancy maps to direct a fixed-width beam toward areas with the highest uncertainty in target presence [4] and to track targets [5]. However, the approaches in [4], [5] do not fully capitalize on the phased array's ability to control the shape of the beam. Recently, in [6], we proposed a spatial beamformer design technique to enhance detection in cells with a higher uncertainty of occupancy. A radar with an analog array that allows both amplitude and phase control at every transmit antenna was assumed in [6] and [7]. Existing automotive radars, however, employ a fully digital MIMO architecture, which grants extra freedom in the waveform design process [8]. As fully digital arrays transmit independent time-domain waveforms from each antenna, they offer superior detection capabilities compared to analog array-based radars, which transmit a single time-domain signal over a beam [9], [10]. When occupancy information about the environment is available, the space-time waveform can be optimized to enhance detection in the areas where the presence of targets is uncertain.

In this paper, we design space-time waveforms for a fully digital automotive MIMO radar by exploiting prior information in the form of occupancy maps and drivable space maps. Our situation-aware waveform design techniques in [6] designed spatial beamformers and ignored time-domain sequence design. This work extends our entropy-based beamformer design formulation in [6] to design situation-aware space-time codes. We consider 2D range-angle matched filtering at the receiver and focus on the transmit waveform design. We propose space-time separable transmit codes where the spatial beams are designed to focus power on regions of high uncertainty of occupancy, while the time-domain codes are designed to enhance target detection within the drivable space. In typical automotive settings, our space-time codes differ substantially from prior agnostic codes employing quasi-omnidirectional beams and time-domain sequences with low autocorrelation properties. We select 100 lane topologies at random from the nuScenes public dataset [11] and consider the case where multiple targets are located along each direction. For these scenarios, we show that our proposed technique outperforms prior agnostic space-time codes that do not leverage any occupancy map information.

II. System model

We consider an automotive radar with a co-located transmitter (TX) and receiver (RX). We assume half-wavelength spaced uniform linear arrays with $N_{\rm tx}$ antennas at the TX and $N_{\rm rx}$ antennas at the RX. Furthermore, we consider fully digital architectures at the TX and the RX as shown in Fig. 1.

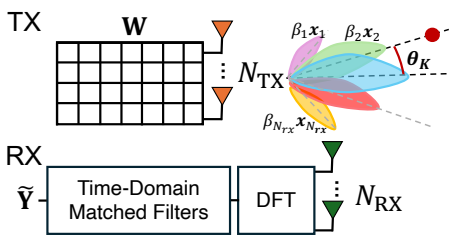

Fig. 1: We design situation aware space-time waveforms for a MIMO radar assuming equal transmit and receive antennas. Here, a time-domain code $\mathbf{x}_i$ is transmitted along direction i with a beamforming gain β_i. In this paper, the β_is and $\mathbf{x}_i$s are tailored to the environment using information from occupancy map and drivable range map.

We assume that the TX periodically transmits a burst of L pulses in one radar coherent processing interval (CPI). Here, L denotes the sample length of the base-band waveform transmitted at each TX element in a CPI. We use P_{tx} to denote the power transmitted by the TX. The transmitted signal impinges K point targets within the radar's field of view. We denote θ_k as the direction of departure associated with the k^{th} target. The array response vector for the half-wavelength spaced TX array for direction θ is defined as

$$\mathbf{a}_{N_{\text{tx}}}(\theta) = [1, e^{\text{j}\pi\sin\theta}, e^{2\text{j}\pi\sin\theta}, \cdots, e^{\text{j}\pi(N_{\text{tx}}-1)\sin\theta}]^T. \quad (1)$$

At the radar receiver, the reflected radar echoes are down-converted and sampled. The matrix of observed measurements in a CPI of M units can be written as

$$\mathbf{Y} = \sqrt{P_{\text{tx}}} \sum_{k=1}^{K} \frac{\alpha_k}{d_k^2} \mathbf{a}^*_{N_{\text{rx}}}(\theta_k) \mathbf{a}^H_{N_{\text{tx}}}(\theta_k) \mathbf{W}_{d_k} + \mathbf{V} \quad (2)$$

where d_k is the range associated with the k^{th} target and $\mathbf{V}$ is the additive circular Gaussian noise in the observed measurements. Further, $\mathbf{W}_{d_k} \in \mathbb{C}^{N_{\text{tx}} \times M}$ is the delayed version of the $N_{\text{tx}} \times L$ transmitted space-time waveform $\mathbf{W} \triangleq [\mathbf{w}_1, \mathbf{w}_2, \ldots, \mathbf{w}_L]$. The vector $\mathbf{w}_\ell$ within $\mathbf{W}$ is the spatial code applied by the TX at the fast-time instant ℓ. We define c_k as the range bin of the k^{th} target, equivalently c_k is the discrete-time propagation delay proportional to $2d_k$. Then, $\mathbf{W}_{d_k} = [\mathbf{0}_{N_{\text{tx}} \times c_k}, \mathbf{W}, \mathbf{0}_{N_{\text{tx}} \times (M-L-c_k)}]$. Finally, α_k is proportional to the radar cross section (RCS) of the target. The received measurement in (2) encodes the range-angle information of all the K targets.

The received measurements are processed using a matched filter to estimate the DoA and the range of the K targets. First, the receiver extracts the returns from each direction by applying a discrete Fourier transform (DFT)-based matched filter. We define $\mathbf{U}_{N_{\text{rx}}}$ as the $N_{\text{rx}} \times N_{\text{rx}}$ DFT matrix and the angle-domain matched filter output as $\bar{\mathbf{Y}} = \mathbf{U}_{N_{\text{rx}}} \mathbf{Y}$. We assume that the K targets are positioned on the discrete grid described by the columns of the DFT matrix. Under this assumption, θ_ks are such that $\pi\sin\theta_k$ is an integer multiple of $2\pi/N_{\text{rx}}$. The output of the angle-domain matched filter for direction θ_i with $i = 1, \ldots, N_{\text{rx}}$, can be expressed as

$$\bar{\mathbf{Y}}[i,:] = \sqrt{P_{\text{tx}}} \sum_{K=1}^{K_i} \frac{\alpha_k}{d_k^2} \mathbf{a}^H_{N_{\text{tx}}}(\theta_i) \mathbf{W}_{d_k} + \bar{\mathbf{V}}[i,:], \quad (3)$$

where K_i is the number of targets present in the direction θ_i and $\bar{\mathbf{V}} = \mathbf{U}_{N_{\text{rx}}} \mathbf{V}$. Then, time-matched filtering is performed over $\bar{\mathbf{Y}}[i,:]$ to estimate the range of the targets along θ_i.

We now discuss our assumption on the structure of $\mathbf{W}$ that allows our approach to decouple space- and time-domain code optimization. We consider $N_{\text{rx}} = N_{\text{tx}}$ and define

$$\mathbf{W} = \frac{1}{N_{\text{rx}}} (\beta_1 \mathbf{a}_{N_{\text{rx}}}(\theta_1) \mathbf{x}_1^T + \cdots + \beta_{N_{\text{rx}}} \mathbf{a}_{N_{\text{rx}}}(\theta_{N_{\text{rx}}}) \mathbf{x}_{N_{\text{rx}}}^T), \quad (4)$$

where $\mathbf{x}_i \in \mathbb{C}^L$ is the time-domain code transmitted along i^{th} direction and β_i is the beamforming gain used to scale the standard DFT beamformer $\mathbf{a}_{N_{\text{rx}}}(\theta_i)$ in that direction. Under these assumptions, the angle-domain matched filter output can be rewritten as

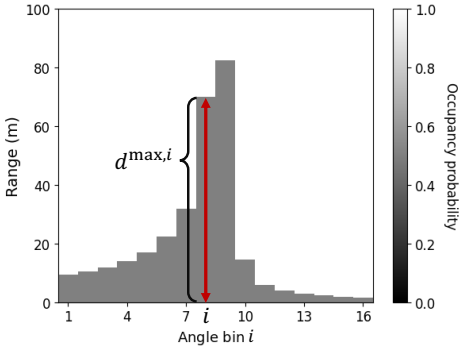

Fig. 2: Occupancy grid map from scene 775 of the nuScenes dataset. Here, z_i denotes the index of the range bin associated with $d^{\max,i}$, the maximum drivable distance along the i^{th} direction.

$$\bar{\mathbf{Y}}[i,:] = \sqrt{P_{\text{tx}}} \sum_{k=1}^{K_i} \frac{\alpha_k}{d_k^2} \beta_i \mathbf{x}_{i,c_k}^T + \tilde{\mathbf{V}}[i,:], \quad (5)$$

where $\mathbf{x}_{i,c_k}^T$ is the delayed version of $\mathbf{x}_i$, i.e., $\mathbf{x}_{i,c_k}^T = [\mathbf{0}_{1\times c_k}, \mathbf{x}_i, \mathbf{0}_{1\times(M-L-c_k)}]$. We observe that the i^{th} row of $\bar{\mathbf{Y}}$ contains only the returns from the i^{th} direction. The RX applies a time-domain matched filter $\mathbf{x}_i$ to retrieve range information of targets along the i^{th} direction. When the $(i,j)^{\text{th}}$ angle-range bin contains a target indexed k, the output of the matched filter is then

$$\tilde{\mathbf{Y}}[i,j] = \sqrt{P_{\text{tx}}} \frac{\alpha_k \beta_i \mathbf{r}_{\mathbf{x}_i}[0]}{d_k^2} + \\ + \sum_{p \in [K_i] \setminus k} \frac{\alpha_p \beta_i \mathbf{r}_{\mathbf{x}_i}[c_p - c_k]}{d_p^2} + \tilde{v}_{\text{filt}}(i,j), \quad (6)$$

where $\tilde{v}_{\text{filt}}(i,j)$ is Gaussian noise obtained by filtering $\tilde{\mathbf{V}}[i,:]$ with $\mathbf{x}_i$. Here, $\mathbf{r}_{\mathbf{x}_i}$ is the autocorrelation of $\mathbf{x}_i$, defined as $\mathbf{r}_{\mathbf{x}_i}[n] = \sum_\ell^L \mathbf{x}_i[\ell] \mathbf{x}_i^*[\ell - n]$, where the scalar $\mathbf{x}_i[\ell]$ is the ℓ^{th} entry of $\mathbf{x}_i$. The second term in (6) represents the contribution of different targets within the same angle bin to the matched filter output. This term can deteriorate target detection capability and should be minimized by designing time-domain codes that have low auto-correlation levels [12], [13].

III. Situation-aware MIMO waveform design

To design the space-time code $\mathbf{W}$ at the TX, we assume that the 2D occupancy map $\mathbb{P}$, defined over the range-angle bins, is known. Here, $\mathbb{P}(i,j)$ denotes the probability that there is a target in the $(i,j)^{\text{th}}$ bin. Fig. 2 shows an example of an occupancy map obtained from the nuScenes dataset [11]. We also assume that the drivable range map, which represents the distance to the closest static obstacle along each direction, is known [7]. For a given static lane topology, let $d^{\max,i}$ represent the distance to the nearest static obstacle along the i^{th} direction, and let z_i denote the index of the range bin corresponding to $d^{\max,i}$. The distance $d^{\max,i}$ refers to the space between the vehicle and the closest boundary (e.g., buildings, guardrails) in each direction of the angular grid. We design $\mathbf{W}$ to maximize the detection probability, especially in

cells in the drivable space that are associated with a higher uncertainty of the target occupancy.

We now formulate optimization problems to design $\mathbf{W}$ from $\mathbb{P}$ and $\{z_i\}_{i=1}^{N_{\mathrm{rx}}}$. We assume that α_k follows a complex Gaussian distribution. For a complex Gaussian α_k, the second summand in (6) is also Gaussian, and we can obtain an expression for the probability of detection by applying the Neyman-Pearson theorem. For our design, we assume that α_k has a unit variance for simplicity. In a practical scenario, α_k can be set assuming the worst-case RCS of the targets in the radar's field of view. When a Neyman-Pearson detector is applied over the model in (6), the probability of detecting a target indexed k in the $(i,j)^{\mathrm{th}}$ bin is [6]

$$P_{\mathrm{d}}(i,j;\{\beta_i\}_{i=1}^{N_{\mathrm{rx}}},\{\mathbf{x}_i\}_{i=1}^{N_{\mathrm{rx}}}) = Q\Bigg(Q^{-1}(P_{\mathrm{FA}}) - \sqrt{\frac{\frac{P_{\mathrm{tx}}}{d_i^4}|\beta_i \mathbf{r}_{\mathbf{x}_i}[0]|^2}{\sigma^2 + \sum_{p\neq k}^{K_i} \frac{P_{\mathrm{tx}}|\beta_i \mathbf{r}_{\mathbf{x}_i}[c_p]|^2}{d_p^4}}}\Bigg), \quad (7)$$

where the term under square root represents the ratio between the signal power in (6) and the noise power. Here, the noise power is the sum of the thermal noise power and the power of the contribution to the matched filter output due to the returns from other cells in the same direction as the target k. As $Q(\cdot)$ is an increasing function, the probability of detection grows with the ratio between the signal power and the sum of the power of the noise plus the power of the contribution to the matched filter output due to returns from targets within the same angle bin as the target k.

In our prior work [6], we showed how to design beamformers from $\mathbb{P}$ for an analog array-based radar. Our approach maximized the weighted probability of detection across different cells, where the weight was set to the entropy of occupancy probability at the cell. The entropy of the occupancy probability measures the uncertainty of a target being present in a cell of interest. In this paper, we still use entropy-based weighted probability of detection. The solution proposed in this paper extends our approach in [6] by also incorporating the impact of time-domain codes in detection. We write the problem of maximizing the weighted detection probability as

$$\begin{aligned}\max_{\{\beta_i,\mathbf{x}_i\}_{i=1}^{N_{\mathrm{rx}}}} & \sum_{i=1}^{N_{\mathrm{rx}}}\sum_{j}^{z_i} H(\mathbb{P}(i,j))P_{\mathrm{d}}(i,j;\{\beta_i\}_{i=1}^{N_{\mathrm{rx}}},\{\mathbf{x}_i\}_{i=1}^{N_{\mathrm{rx}}}) \\ \text{s.t.} & \sum_{i=1}^{N_{\mathrm{rx}}} |\beta_i x_i[\ell]|^2 \leq 1 \quad \forall \ell = 1,\ldots,L,\end{aligned} \quad (8)$$

where $H(\cdot)$ is the information entropy function given by

$$H(p) = -p\log_2(p) - (1-p)\log_2(1-p). \quad (9)$$

The constraint in (8) ensures the radiated power is limited, i.e., $\|\mathbf{w}_\ell\|_2^2 \leq 1\,\forall \ell = 1,\ldots,L$. For a waveform with the structure in (4), it holds that

$$\|\mathbf{w}_\ell\|_2^2 = \frac{1}{N_{\mathrm{rx}}}\|\sum_{i=1}^{N_{\mathrm{rx}}} \beta_i \mathbf{a}_{N_{\mathrm{rx}}}(\theta_i)\mathbf{x}_i[\ell]\|_2^2 = \sum_{i=1}^{N_{\mathrm{rx}}} |\beta_i \mathbf{x}_i[\ell]|^2,$$

where the last equality follows from the orthogonality of the DFT matrix. The power constraint then reduces to $\sum_i |\beta_i \mathbf{x}_i[\ell]|^2 \leq 1\,\forall \ell$. The maximization problem in (8) is a non-concave problem with a non-convex constraint [6].

We propose a greedy two-step approach to obtain a feasible solution for (8). In the first step, we ignore the second summand in (6) by considering ideal time-domain codes. Under this assumption, P_{d} in (7) depends only on the beamforming gains $\{\beta_i\}_{i=1}^{N_{\mathrm{rx}}}$. The relaxed problem in our first step thus reduces to

$$\begin{aligned}\max_{\{\beta_i\}_{i=1}^{N_{\mathrm{rx}}}} & \sum_{i=1}^{N_{\mathrm{rx}}}\sum_{j=1}^{z_i} H(\mathbb{P}(i,j))P_{\mathrm{d}}(i,j;\{\beta_i\}_{i=1}^{N_{\mathrm{rx}}}) \\ \text{s.t.} & \sum_{i=1}^{N_{\mathrm{rx}}} |\beta_i x_i[\ell]|^2 \leq 1 \quad \forall \ell = 1,\ldots,L.\end{aligned} \quad (10)$$

We note that the constraint in (10) depends on the design of the time-domain codes. To make the constraint in (10) independent of the design of $\mathbf{x}_i$s, we consider unimodular time-domain codes, i.e., $|\mathbf{x}_i| = \mathbf{1}$, where $\mathbf{1}$ is the all-ones vector of length N_{rx}. The constraint in (10) then becomes $\sum_i^{N_{\mathrm{rx}}} |\beta_i|^2 \leq 1\,\forall \ell$ and (10) is solved using projected gradient ascent to obtain the optimized β_i's.

In the second step, the time-domain $\mathbf{x}_i$'s are optimized to minimize the noise term in (7) due to the returns from targets in the same direction as the cell of interest. Targets may exist up to the drivable distance $d^{\max,i}$ along direction i. To reduce the contribution from different cells along the i^{th} direction, we minimize the autocorrelation $\mathbf{r}_{\mathbf{x}_i}$ for the lags less than z_i, expressed as,

$$\min_{\{\mathbf{x}_i\}_{i=1}^{N_{\mathrm{rx}}}} \sum_{\ell=-(z_i-1)}^{z_i-1} |\mathbf{r}_{\mathbf{x}_i}[\ell]|^2 \quad \text{s.t.} \quad |\mathbf{x}_i| = \mathbf{1} \;\; \forall i = 1,\ldots,N_{\mathrm{rx}}. \quad (11)$$

Our formulation in (11) ignores returns from targets outside the drivable region. In practice, these returns may stem from static obstacles like buildings or lamp posts located beyond z_i. Our solution can still be used in such scenarios by employing static clutter removal techniques [14] to eliminate these returns. Solving (11) results in sequences that reduce the contribution from other cells in the drivable region along the i^{th} direction. The problem of designing low correlation sequences has been widely studied in the literature [12], [13]. In this paper, we apply the method from [13] to solve (11) for each i. After computing β_i and $\mathbf{x}_i$, the space-time code is given by (4).

IV. Simulation results

To evaluate the proposed approach, we solve the optimization problem in (8) and compare detection performance of the proposed space-time code with a code that is agnostic to prior occupancy information. We use $N_{\mathrm{tx}} = 16$ TX antennas and $N_{\mathrm{rx}} = 16$ RX antennas, assuming perfect amplitude and phase control at all the elements of the TX array. We consider a bandwidth of $750\,\mathrm{MHz}$, which results in a range resolution of $0.20\,\mathrm{m}$. The maximum range across all directions is set to $200\,\mathrm{m}$, which corresponds to 1000 range bins.

In our evaluation, we use lane topology maps from the nuScenes dataset [11] to construct occupancy grid maps such

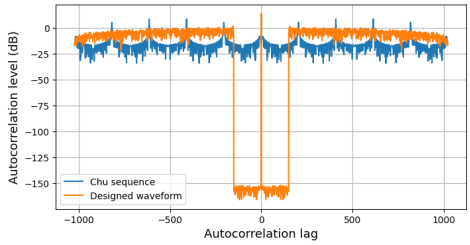

(a)

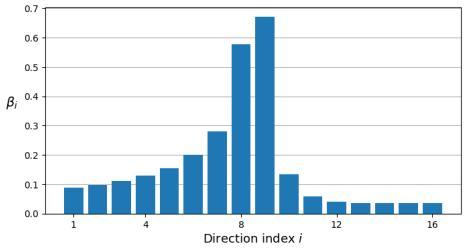

(b)

Fig. 3: In (a) we compare the autocorrelation of the designed waveform using the algorithm in [13] with that of a Chu sequence. The designed waveform minimizes correlation at the difference of range bin indices within the drivable space. In (b), we show the beamforming gains, the β_is, for the lane topology in Fig. 2. These gains $\{\beta_i\}_{i=1}^{N_{\text{rx}}}$, used to scale the standard DFT beamformers, are constructed using prior lane topology information.

as the one in Fig. 2. The nuScenes dataset contains labels for the plausible drivable space for several driving scenes. We consider the cells within the drivable space to have unknown occupancy ($\mathbb{P}(i,j) = 0.5$) and the cells outside of it to be occupied by static objects such as buildings and have certain occupancy ($\mathbb{P}(i,j) = 1$).

Fig. 3a shows the autocorrelation of the time-domain waveform designed using (11) for the direction indexed 7 in 2. Here, the maximum distance at which the target could be located is around 30 meters, which corresponds to $z_7 = 150$ range bins. We compare the autocorrelation of the designed sequence with that of a Chu sequence, a code that does not leverage any side information on the scene. The time-domain sequence designed using drivable range information achieves autocorrelation levels up to 125 dB less in magnitude when compared to the Chu sequence for the lags within z_i. As a result, the impact of other targets within the same angle bin is minimized in detection using the time-domain matched filter. The low correlation for lags within z_i also contributes to suppressing the contribution of clutter in the considered angle bin [12]. We also observe from Fig. 3a that the designed waveform exhibits a higher correlation than the Chu sequence beyond the lag of z_i. Due to such high correlation, targets in the drivable space can lead to ghost targets outside the drivable space. These ghost artifacts are usually irrelevant as they occur beyond the drivable space. Finally, targets in range bins between z_i and $2z_i$ influence detection within the drivable space due to the high autocorrelation beyond z_i in our design. We assume that the returns from those targets can be mitigated using clutter cancellation techniques.

Next, we demonstrate the improved detection capabilities of the proposed space-time waveform design for 100 scenes of the nuScenes dataset. Here, we use the beamforming gains designed with our approach together with the designed time-domain codes. The baseline space-time code uses uniform β_is and Chu codes. For each of the considered scenes, we suppose that 5 targets are located at random distances from the radar along each grid direction. These targets have a random RCS, such that each α_k is sampled from a Gaussian distribution with a variance of $-57\,\text{dB}$. Additionally, we set the transmitted power to $10\,\text{dB}$ and the variance of the thermal noise at the receiver to $-115\,\text{dB}$. For each scene, the experiments are repeated for 20 random placements of the targets. Fig. 4 shows the boxplot of the probability of detection obtained using a Chu sequence with uniform β_is and the proposed design for different values of P_{FA}. The proposed approach achieves a higher median probability of detection than the one using Chu sequences. In particular, for a P_{FA} of 10^{-4} we observe a 0.9 higher probability of detection. Due to the higher correlation for lags less than z_i, the Chu waveform results in a significant noise at the matched filter output due to the presence of multiple targets within the same angle bin as the target of interest. This results in a lower median detection rate than the one achieved by the proposed situation-aware approach. By minimizing the time-domain autocorrelation function within z_i, the proposed approach can reliably detect multiple targets within the same angle bin than a standard method.

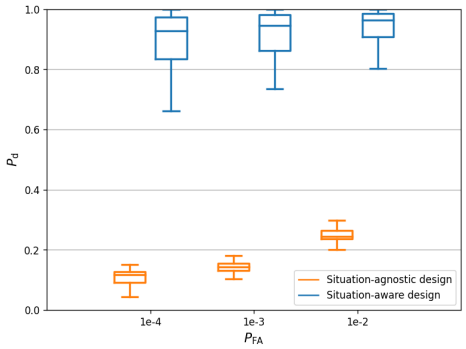

Fig. 4: We show the boxplot of the detection probability for 100 lane topologies. We compare the situation-aware design (using optimized $\mathbf{x}_i$s and β_is) and the standard situation agnostic design (employing Chu sequences and uniform β_is). We observe that Our method achieves better median detection probability by exploiting prior information.

V. Conclusions

In this paper, we develop a space-time design technique for automotive radars using a fully digital MIMO architecture. Our design incorporates prior information, in the form of occupancy maps and drivable space maps, in the waveform design process. Our method optimizes a separable space-time code where the spatial beams focus power in the regions of uncertain target presence and the time codes enhance the detection of multiple targets within the same angle bin. Simulation results over the nuScenes dataset indicate that our adaptive space-time code achieves higher probability of detection for a fixed probability of false alarm, when compared to space-time codes that do not exploit prior information.

REFERENCES

[1] Z. Zhang, T. Wang, S. Gu, and Z. Xiang, "MPF: a robust vehicle localization framework based on topological map and odometry," *IEEE Sens. J.*, vol. 23, no. 7, pp. 7242–7252, 2023.

[2] Ç. Önen, A. Pandharipande, G. Joseph, and N. J. Myers, "Occupancy grid mapping for automotive driving exploiting clustered sparsity," *IEEE Sens. J.*, vol. 24, no. 7, pp. 9240–9250, 2024.

[3] F. Gies, A. Danzer, and K. Dietmayer, "Environment perception framework fusing multi-object tracking, dynamic occupancy grid maps and digital maps," in *Proc. Int. Conf. Intell. Transp. Syst. (ITSC)*, 2018, pp. 3859–3865.

[4] R. A. Romero and N. A. Goodman, "Cognitive radar network: Cooperative adaptive beamsteering for integrated search-and-track application," *IEEE Trans. on Aero. and Elec. Sys.*, vol. 49, no. 2, pp. 915–931, 2013.

[5] Z. W. Johnson and R. A. Romero, "Adaptive beamsteering cognitive radar with integrated search-and-track of swarm targets," *IEEE Access*, vol. 9, pp. 50 652–50 666, 2021.

[6] E. Focante, N. J. Myers, G. Joseph, and A. Pandharipande, "Situation-aware adaptive transmit beamforming for automotive radars," in *Proc. IEEE Int. Conf. Acoust. Speech Signal Process. (ICASSP)*, 2024.

[7] ——, "Adaptive beamforming for situation-aware automotive radars under uncertain side information," *IEEE Trans. Radar Sys.*, vol. 2, pp. 699–711, 2024.

[8] S. Sun, A. P. Petropulu, and H. V. Poor, "MIMO Radar for Advanced Driver-Assistance Systems and Autonomous Driving: Advantages and Challenges," *IEEE Signal Processing Magazine*, vol. 37, no. 4, pp. 98–117, 2020.

[9] W. Wu, R. B. Staszewski, and J. R. Long, "A 56.4-to-63.4 GHz Multi-Rate All-Digital Fractional-N PLL for FMCW Radar Applications in 65 nm CMOS," *IEEE Journal of Solid-State Circuits*, vol. 49, no. 5, pp. 1081–1096, 2014.

[10] J. Hasch, "Driving towards 2020: Automotive radar technology trends," in *2015 IEEE MTT-S International Conference on Microwaves for Intelligent Mobility (ICMIM)*, 2015, pp. 1–4.

[11] H. Caesar, V. Bankiti, A. H. Lang, S. Vora, V. E. Liong, Q. Xu, A. Krishnan, Y. Pan, G. Baldan, and O. Beijbom, "nuScenes: A multimodal dataset for autonomous driving," in *Proc. IEEE/CVF Conf. Comput. Vis. Pattern Recognit. (CVPR)*, 2020, pp. 11 621–11 631.

[12] P. Stoica, H. He, and J. Li, "New algorithms for designing unimodular sequences with good correlation properties," *IEEE Transactions on Signal Processing*, vol. 57, no. 4, pp. 1415–1425, 2009.

[13] J. Song, P. Babu, and D. P. Palomar, "Sequence design to minimize the weighted integrated and peak sidelobe levels," *IEEE Transactions on Signal Processing*, vol. 64, no. 8, pp. 2051–2064, 2016.

[14] W. W. Shrader and V. Gregers-Hansen, "MTI radar," *Radar Handbook*, vol. 2, pp. 15–1, 1970.